Kink dynamics in finite discrete sine-Gordon chains

Artur Kwaśniewski, Paweł Machnikowski,* and Piotr Magnuszewski
Institute of Physics, Wrocław University of Technology, Wybrzeże Wyspiańskiego 27, 50-370 Wrocław, Poland
(Received 19 June 1998; revised manuscript received 21 September 1998)

The dynamics of one-dimensional finite discrete sine-Gordon (Frenkel-Kontorova) chains is studied for small values of misfit. It is shown that nonintegrability leads to kink trapping at the system surface, stopping the system motion as a whole and localizing energy at the system boundary. An interpretation from the point of view of both dislocation dynamics and proton transport is proposed. [S1063-651X(99)00402-X]

PACS number(s): 36.20.−r, 45.05.+x, 63.20.Ry

I. INTRODUCTION

Simple models of complex microscopic nonlinear phenomena have been used for several decades in various branches of solid state physics (e.g., Refs. [1–3]). Recently they have also been very popular in the description of nonlinear transport phenomena in hydrogen bonded chains both in condensed matter and in living systems [4–7]. Such models are expected to reveal fundamental features of real systems, allowing, at the same time, for analytical or relatively simple numerical treatments. An analysis of any such model not only contributes to the knowledge of a specific system, but also helps in understanding the general theory of nonlinear systems.

One of widely used models is the Frenkel-Kontorova (FK) model [1], whose finite version with free ends is defined by the Hamiltonian (in dimensionless units)

$$H=\tfrac{1}{2}\sum_{n=1}^{N} p_n^2+\sum_{n=1}^{N} V_0(1-\cos u_n)+\tfrac{1}{2}\sum_{n=1}^{N-1}(u_{n+1}-u_n-a)^2, \tag{1}$$

where u_n and $p_n=\dot{u}_n$ are position and momentum of the nth node, respectively, and a is the misfit between the chain lattice constant and the substrate period.

The dynamical equations for system (1) have the forms

$$\ddot{u}_1-(u_2-u_1-a)+V_0\sin u_1=0,$$

$$\ddot{u}_n-\Delta_2 u_n+V_0\sin u_n=0, \quad 2\leqslant n\leqslant N-1,$$

$$\ddot{u}_N+(u_N-u_{N-1}-a)+V_0\sin u_N=0,$$

where $\Delta_2 u_n=u_{n+1}-2u_n+u_{n-1}$. The continuum limit of the infinite version of this model—the sine-Gordon (SG) equation—is exactly solvable; formulas for fundamental classes of solutions may be obtained by inverse scattering technique (see, e.g., Ref. [8]) or by Hirota method [9,10].

The importance of system finiteness was noted a long time ago by Frank and van der Merwe [2] and Kovalev [11], who analyzed the FK model of dislocations in crystals, as well as by Costabile *et al.* [12] in the study of Josephson transmission lines. Certain new aspects and applications were described by Pawełek [13] and Kukushkin and Osipov [14]. However, all those investigations concerned the continuum limit of the model.

Discreteness in a finite system was taken into account by Markov and Karaivanov [15] and Braun [16] who analyzed the static configurations of the FK model and the most favorable energetic paths joining them. Sharma, Bergsen, and Joos [17] and Braiman *et al.* [18] studied the Aubry transition in a finite system, showing that its character is different from the continuum case. Stoyanov and Müller-Krumbhaar [19] analyzed the dynamics of linear modes around equilibrium configurations, and showed that resonance with external fields may lead to Brownian motion of a system (as a whole) over the substrate. All these works deal with static configurations or adiabatic motion.

On the other hand, in a description of biological phenomena discreteness is considered to be essential, and is usually taken into account. However, finiteness effects have not been analyzed so far. One may expect system boundaries to be very important for transport phenomena in real systems.

Meanwhile, it is known that finiteness and discreteness in another class of models (Fermi-Pasta-Ulam type) lead to many interesting dynamical phenomena [20–23]. All this indicates that for a correct description of the dynamics of a finite discrete system, it is essential to take both these features into account.

In this paper we study the interplay between system finiteness and discreteness, analyzing the kink dynamics in a FK chain. We limit ourselves to the case of small misfit. The limit of $a=0$ is analyzed in detail providing basis for more general conclusions. We show that including nonintegrability (here resulting from discreteness) in a description of finite systems (i.e., in a model discussed, e.g., by Kovalev [11] and Kukushkin and Osipov [14]) leads to qualitative effect on system dynamics. In particular, we point out that in a wide range of system parameters a kink in a discrete chain may move almost freely along the chain, while during reflection from the chain end the radiation is strong enough to for the kink to get trapped.

In spite of using the special model (1) as a background for the presented discussion, the phenomena described in the following sections are general, and can be expected in a wide class of related systems. The paper is organized as follows.

In Sec. II, we review the results concerning the dynamics of a finite continuous SG system with free boundary condi-

*Author to whom correspondence should be addressed. Electronic address: machnik@rainbow.if.pwr.wroc.pl

tions. The dynamics of a discrete SG (FK) chain with free boundary conditions is discussed in Sec. III: Discreteness is treated by the collective variable approach in Sec. III A, leading to previsions concerning the dynamics of a finite discrete system. The previsions are verified by the numerical results in Sec. III B. Discussion of the general results of these sections from the point of view of specific applications is contained in Sec. IV. Section V contains a summary, and outlooks for further study.

II. CONTINUOUS SYSTEMS

The dynamics of an infinite continuous SG system may be studied by means of the inverse scattering transform, leading to exact general solutions. These results may be directly applied to finite or semi-infinite chains. Such an idea was first proposed by Frank and van der Merwe [2] who noticed that cutting the system at a zero-tension point does not influence its equilibrium.

When the dynamics of a finite SG systems is considered, exact results may be obtained for $a=0$ using the equivalence between a semi-infinite or finite chain and an infinite chain, with a proper symmetry of the initial conditions. Symmetric solutions for the SG equation were first used to describe the dynamics of a finite chain by Costabile *et al.* [12] and Kovalev [11]. The idea was also used in Ref. [24] to simplify numerical simulations of symmetric collisions of kinks and breathers. It is applicable to other classes of nonlinear models, as well (see, e.g., Ref. [25]).

Below we briefly review results for a semi-infinite system, assuming that the system is long enough to neglect the opposite end. This is justified since the kink width is usually equal to a few lattice constants, while chains involved in many physical situations are much longer. Note also that if the kink width is comparable to the chain length, the kink's identity becomes vague and one deals with a completely different dynamics.

Formally, for any initial state of the system satisfying

$$u'(x)|_{x=0^+}=0, \tag{2}$$

the dynamics is equivalent to the dynamics of an infinite system with a smooth, symmetric, initial condition

$$u(-L)=u(L), \quad \dot{u}(-L)=\dot{u}(L).$$

The dynamics of the SG model involving nonsmooth field states is a rather unusual problem. In fact, all cases of localized excitations approaching the chain end from a large enough distance satisfy the smoothness condition (2).

Following the exhaustive analysis of Kovalev [11] (see also generalization of these results by Pawełek [26]), one may, according to the above equivalence, distinguish two regimes of kink dynamics in a semi-infinite system: (1) Localized surface excitations, i.e., bound states of a kink at the system boundary, corresponding to SG breathers in the infinite system. (2) Free kink movement corresponding (in a long enough chain) to a collision of the kink with its mirror image (an antikink moving with opposite velocity); the collision is centered at $x=0$. After the collision the kink transforms into an antikink and escapes to ''infinity.''

The essential point is that the reflection does not change the form, energy, or velocity of the kink, except for transforming it into an antikink. In the integrable, continuum case the kink dynamics is strictly conservative. Due to energy conservation and the elasticity of interactions, a transition from the free movement to the bound surface state is impossible.

III. DISCRETE SYSTEMS

In this section we will consider the dynamics of a semi-infinite discrete chain in the limit $a=0$. We will use a straightforward generalization of the approach presented in Sec. II.

The system consisting of nodes $n=1,2,\ldots$ may be considered as one half of an infinite *extended system*. Any initial condition having the symmetry

$$u_{-n}=u_{n+1}, \quad \dot{u}_{-n}=\dot{u}_{n+1}, \quad n=1,2,\ldots \tag{3}$$

will evolve conserving this symmetry (a formal proof of this intuitively obvious fact is given in the Appendix). Since $u_1=u_0$, the first node will not ''feel'' any force from its left neighbor. Therefore, the two parts of the chain actually do not interact (although we speak of the interaction of colliding kinks), and we have a zero-tension point at any moment of time, corresponding to the ideas of Frank and van der Merwe [2].

The Poynting energy flow between the nodes 0 and 1 is

$$P_{0,1}=\frac{1}{2}(u_1-u_0)(\dot{u}_1+\dot{u}_0)=0.$$

Hence, there is no energy flow between the real and fictitious part of the chain, and the energy of the real chain is conserved and equal to half the energy of the extended system.

A. Adiabatic effective potential

To understand the kink dynamics in a semi-infinite discrete chain, it is very useful to analyze the effective potential for the kink using the collective variable method. Compared to more general (applicable for $a\neq 0$) and more exact numerical methods [15,16], this has the advantage of tracing explicitely the kink position and yielding closed analytical formulas.

It is possible to apply the collective variable method directly to a finite system. However, both idea and notation become more clear if the correspondence with the infinite system is applied to reduce the problem to that of discrete kink-antikink interaction in an infinite chain.

The SG breather dynamics in the discrete system was studied by Boesch and Peyrard in Ref. [27]. In that paper the dynamics of moving subkinks bound in a SG breather was studied, but the complexity of the dynamical problem allowed the authors to obtain analytical solutions only in the bare kink approximation, i.e., no corrections (either localized or radiative) to the continuous ansatz were taken into account. Below we use the method proposed by Willis, El-Batanouny, and Stancioff [28], and calculate the effective potential for the kink in a finite system up to the linear adiabatic correction. Then one may assume that a moving kink

corresponds to a particle moving in this potential.

Applying the standard procedure [28], we introduce the additional dynamical variables X, $P=\dot{X}$, related to the position of the kink center, by

$$u_n = f_n(X) + q_n, \quad \dot{u}_n = \dot{X} f_n'(X) + p_n,$$

where $p_n = \dot{q}_n$. To keep the number of degrees of freedom unchanged, two constraints must be introduced,

$$C_1 = \sum_n f_n' q_n = 0, \quad C_2 = \sum_n f_n' p_n = 0, \tag{4}$$

where the first one prevents the kink position from being changed by the correction q_n. As an approximation $f_n(X)$ of the kink shape, we use the kink-antikink superposition centered at $n=\frac{1}{2}$:

$$\begin{aligned} f_n(X) &= 4 \arctan \exp[\sqrt{V_0}(n+X-1)] \\ &\quad - 4 \arctan \exp[\sqrt{V_0}(n-X)] \\ &= 4 \arctan\left[\frac{\sinh[\sqrt{V_0}(X-1/2)]}{\cosh[\sqrt{V_0}(n-1/2)]}\right], \end{aligned} \tag{5}$$

which obviously satisfies the symmetry condition (3). Since our procedure involves the assumption that q_n are small, f_n should not be very different from the actual discrete solution, which is true for our choice of f_n except for high discreteness and for kink positions very close to the chain end.

The collective variable Hamiltonian has the form

$$H = \frac{P^2}{2M} + \tfrac{1}{2}\sum_n p_n^2 + V(X, \boldsymbol{q}), \tag{6}$$

where the potential energy is

$$\begin{aligned} V(X,\boldsymbol{q}) = \sum_n \{ &\tfrac{1}{2}(f_{n+1} + q_{n+1} - f_n - q_n)^2 \\ &+ V_0[1 - \cos(f_n + q_n)]\}. \end{aligned}$$

We assume that the correction q_n is small, and expand the potential to the second order in $\boldsymbol{q} = (\ldots, q_{-1}, q_0, q_1, \ldots)$,

$$V \approx V^{(2)} = V(\boldsymbol{f}) - \tfrac{1}{2}\langle \boldsymbol{f}|\Delta_2|\boldsymbol{f}\rangle - \langle \boldsymbol{q}|\boldsymbol{F}\rangle + \tfrac{1}{2}\langle \boldsymbol{q}|A|\boldsymbol{q}\rangle,$$

where the Dirac bracket stands for the usual l_2 scalar product, and the following notation has been used:

$$\boldsymbol{f} = (\ldots, f_{-1}, f_0, f_1, \ldots), \quad \boldsymbol{f}' = \frac{d\boldsymbol{f}}{dX},$$

$$V(\boldsymbol{f}) = \sum_i V(f_i), \quad V_l' = V'(f_l), \quad \mathsf{V}_{ij}'' = V''(f_i)\,\delta_{i,j}$$

(the primes on the right-hand side denote differentiation with respect to the argument of V),

$$[\Delta_2]_{ij} = \delta_{i,j+1} - 2\,\delta_{i,j} + \delta_{i,j-1},$$

$$\mathsf{A} = -\Delta_2 + \mathsf{V}'', \quad \boldsymbol{F} = \Delta_2 \boldsymbol{f} - \boldsymbol{V}'.$$

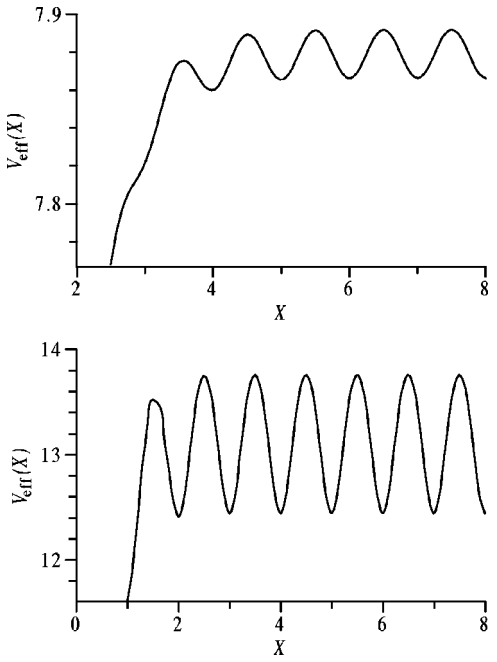

FIG. 1. Effective potential for $V_0=1$ (a) and $V_0=3$ (b).

In order to find the minimum potential energy of the system with the ansatz f_n located at a specific X, one should find the conditional minimum of the effective potential satisfying the constraint $C_1=0$ [28]. To this end we introduce the Lagrange multiplier $\lambda(X)$, and minimize the function

$$\tilde{V}(X,\boldsymbol{q}) = V^{(2)}(X,\boldsymbol{q}) + \lambda(X)\langle \boldsymbol{q}|\boldsymbol{f}'\rangle,$$

with respect to $\boldsymbol{q}$.

A straightforward calculation leads to the following results:

$$\lambda(X) = -\frac{\langle \boldsymbol{F}|\mathsf{A}^{-1}|\boldsymbol{f}'\rangle}{\langle \boldsymbol{f}'|\mathsf{A}^{-1}|\boldsymbol{f}'\rangle}, \quad \boldsymbol{q} = \mathsf{A}^{-1}(\boldsymbol{F} + \lambda \boldsymbol{f}')$$

and

$$V_{\rm eff}(X) = \min_{\boldsymbol{q}} \tilde{V}(X,\boldsymbol{q}) = V(\boldsymbol{f}) - \tfrac{1}{2}\langle \boldsymbol{q}|\Delta_2|\boldsymbol{F}\rangle - \tfrac{1}{2}\langle \boldsymbol{f}|\Delta_2|\boldsymbol{f}\rangle.$$

The effective potential calculated in this way corresponds to the extended system. The potential for the semi-infinite chain is equal to $\frac{1}{2}V_{\rm eff}$.

The effective potential is plotted in Fig. 1. The potential has the usual Peierls-Nabarro form far enough from the chain end, whereas near the end it drops to zero. Hence the kink is attracted by the chain end, as it was in the continuum case. The difference is the periodic modulation of the potential due to discreteness. A similar form of the effective potential was obtained in Ref. [27].

The linear correction is sufficient for obtaining accurate results if its magnitude $\max_n\{q_n\}$ is small enough. We have confirmed that for $V_0<3$ it never exceeds 0.4. The correction is relatively large for $X<5$ due to the fact that the superposition ansatz (5) breaks when the kinks come close to each other, and a considerable correction is neccessary for low values of X. It also increases for $V_0>1$, but only for X very close to integer (kink located on a node). For half-

integer kink positions the linear correction approximation is still reliable even for $V_0>3$. Thus the potential shape obtained with this method is more accurate near its maxima.

B. Dynamical effects

Before we analyze the effect of system finiteness on the dynamics, let us briefly summarize the known properties of kink dynamics in a discrete system (first discussed by Currie *et al.* [29] and later by Willis and co-workers [28,30]). Translational symmetry in the continuum case allows the symmetry-breaking topological solutions to take any of the continuum of equivalent positions in the system. The collective variable in this case corresponds to the symmetry-restoring Goldstone mode of zero energy. In a discrete system, there is no translational symmetry, and the mode related to the collective variable [i.e., the one ruled out by the constraints (4)] has a finite energy gap and is transformed to the Peierls-Nabarro (PN) mode [31]. Globally, it is accepted to describe kinks as particles moving in an effective Peierls-Nabarro potential. Moving discrete kinks radiate energy [29]; the radiation rate is high especially when the natural frequency $\omega_1=2\pi v$ is above the lower edge of the phonon spectrum. Large phonon packets are radiated out when ω_1 crosses the lower edge of the phonon band $\omega_0=\sqrt{V_0}$. Hence any initial kink velocity drops almost immediately below the critical velocity [28],

$$v_c=\frac{\omega_0}{2\pi}. \tag{7}$$

Therefore, only a dynamics with velocities below the critical one is of practical importance. A higher initial velocity will lead only to a higher radiation background, which will introduce noise effects into kink dynamics. We will not study this issue here.

One may expect two important effects related to the potential well at the chain end. First, since reflection from the system boundary corresponds to a kink-antikink collision and the latter is not perfectly elastic in a nonintegrable system, reflection should be accompanied by strong radiation. Second, we expect that the effective potential well at the system end should lead to a kink trapping effect at the system boundary, analogous to the pinning in a PN well, due to energy loss.

Hence we expect that near the continuum limit (displacive case) the kink dynamics will not differ considerably from the continuum case. The energy loss will be small, both in the bulk and during reflection.

For stronger (compared to the nearest neighbor coupling) potentials—i.e., more discrete systems—a kink will radiate more energy during reflection. It may therefore be expected that any kink will be likely to move from one chain end to the other but most probably will not reflect, staying stuck at the chain end. For still higher discreteness, kinks become pinned in the PN well almost at once [29].

To verify the above ideas, let us study the dynamics of a kink in a SG chain using a numerical simulation. The kink behavior is examined for various values of potential amplitude (discreteness). Interaction with a random phononic background, always present in a nonintegrable system, makes it impossible to draw strict general conclusions on the grounds of numerical results. Nevertheless, it is possible to single out and discuss a number of typical dynamical scenarios depending on the degree of discreteness. The simulations were performed using the SWARM [32] package and the symplectic integration algorithm [33].

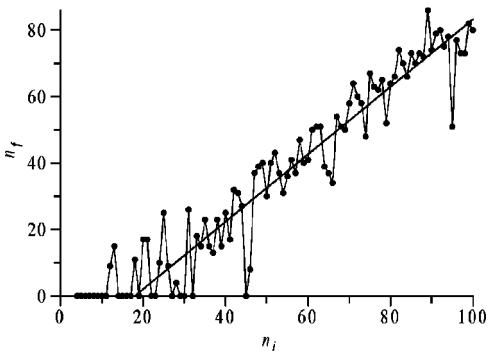

FIG. 2. Dependence between initial (n_i) and final (n_f) positions of a slow kink moving toward the chain end for $V_0=1$, initial velocity $v=-0.01$. The straight line shows the trend obtained by linear regression.

In the first numerical experiment, we examined the influence of the effective potential well at the chain end by launching a slow kink ($v=-0.01$) from various nodes in a chain of medium discreteness ($V_0=1$, $N=200$ nodes). We analyzed the dependence between initial and final kink positions (Fig. 2). To some extent the final position is random, which is caused by collisions with phonons disturbing the kink motion. However, the main trend is clear: in central parts of the chain the kink can travel a distance of approximately 12 nodes before it is pinned in a PN well. On the other hand, the kink is never pinned on one of the first three nodes which belong to the effective potential well at the chain end (see Fig. 1). Moreover, a kink is never reflected, no matter how close to the system boundary it began. All kinks that reach the chain end stay stuck. Hence it is clear that the energy radiated by a kink while reflecting from the chain end (crossing the effective potential well) is much larger than the energy lost over the same distance in the chain.

Our second numerical experiment led to a quantitative estimation of the energy loss due to reflection. We measured the energy radiated by a kink starting from the 20th node of the chain, reflecting and returning to the 20th node. This was compared to the energy radiated by a kink travelling 40 nodes in the central part of a chain with the same initial velocity. The difference may be considered to be energy loss due only to reflection. In this experiment, kink velocities were close to (but lower than) the critical velocity v_c [Eq. (7)] for a given potential amplitude V_0. The results are shown in Fig. 3.

For low potential amplitudes (close to the continuum limit) the kink behaves like in the continuous system. The kink reflects from the chain end undergoes a change into an antikink. The energy loss due to reflection (corresponding to collision with the kink's image) is small and, e.g., for $V_0=0.2$ equals $\Delta\epsilon/\epsilon=0.06\%$. There is only a very weak dependence on the kink velocity. An energy-density graph of the system dynamics in this case is shown in Fig. 4. Very

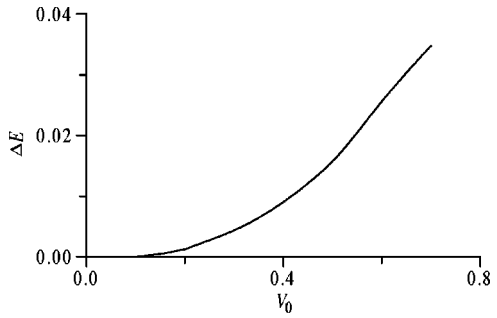

FIG. 3. Energy loss due to reflection from the chain end for various potential amplitudes V_0.

little radiation is produced both during normal traveling and at the moment of reflection. Moreover, in the continuum limit the SG kink does not interact with phonons. Therefore, there are also no effects related to kink-phonon interaction.

Increasing the potential amplitude V_0 results in growing system discreteness. The kink dynamics becomes affected by the PN potential. Nonintegrability results in kink-phonon interaction of two kinds: phonon emission [29,30] and kink-phonon scattering. On the energy-density diagram (Fig. 5) one can see phonon packets radiated at $t=0$ and during reflection ($t=400$). The former is due to a dynamical adjusting of our numerical ansatz to the real kink shape. The latter is much larger, and causes a considerable decrease of the kink energy (cf. Fig. 3), noticeable in Fig. 5 as a lowering of the kink velocity after reflection. The kink-phonon interaction induced by discreteness is also evident, giving rise to a ''sea'' of phononic excitations localized between the kink and the chain end.

From collective variable estimations (Sec. III A) it is clear that the potential well formed at the chain end is much deeper than the PN well (cf. Fig. 1). On the other hand, the energy loss due to an inelastic collision with the kink's image grows much faster than the radiation rate during normal traveling (cf. Fig. 3). For potential amplitudes $V_0 \approx 0.6$, only kinks with velocities higher than a certain threshold have enough energy to reflected, while slower ones stay stuck at the chain end. Finally, for $V_0 \approx 0.8$ the threshold velocity

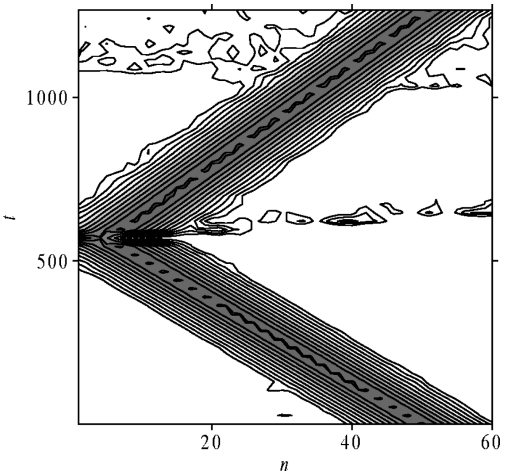

FIG. 4. Energy density diagram of the system dynamics for $V_0=0.3$ and initial kink velocity $v=-0.08$. The gray scale corresponds to the logarithm of the energy density.

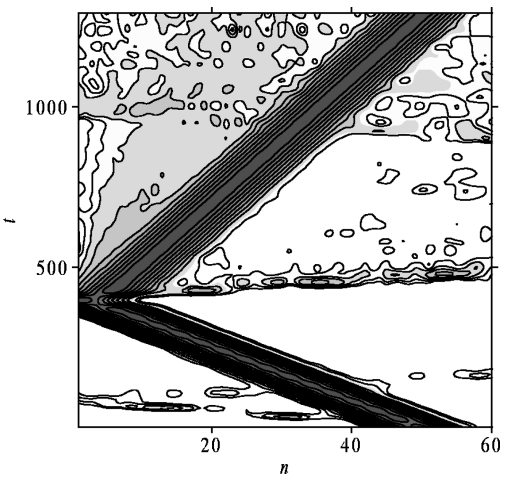

FIG. 5. Energy density diagram of the system dynamics for $V_0=0.6$ and initial kink velocity $v=-0.11$. The gray scale corresponds to the logarithm of the energy density, and is the same as in Fig. 4.

becomes equal to the critical velocity v_c and no kink may be reflected. An example is shown in Fig. 6. Much energy is radiated during reflection, and the kink becomes pinned in the effective potential well at the system end. When the kink oscillates at the chain end, the higher harmonics of its frequency are in resonance with the phonon spectrum, which results in strong radiation, clearly seen in Fig. 6.

IV. DISCUSSION

As shown in the preceding sections, discreteness strongly modifies the dynamics of a finite SG system. In a continuous system a kink moves in a periodic way with perfectly elastic reflections from the system boundaries (surfaces). Each period of kink motion results in shifting the system, as a whole, by two substrate periods. Conversely, in a discrete system the kink is very likely to be trapped at the surface. For large enough discreteness ($V_0>0.8$), no kink traveling with an allowed velocity $v<v_c$ may be reflected from the system

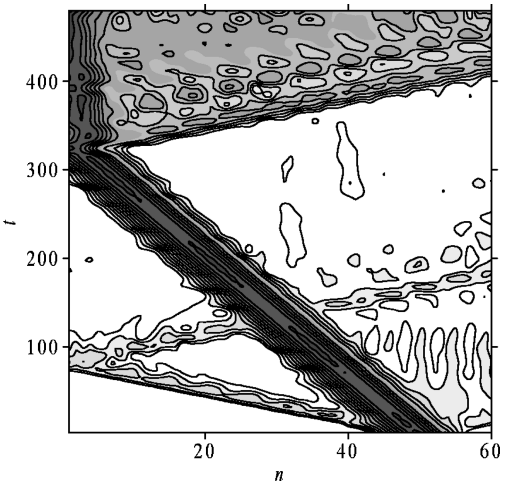

FIG. 6. Energy density diagram of the system dynamics for $V_0=1$ and initial kink velocity $v=-0.14$. The gray scale corresponds to the logarithm of the energy density, and is the same as in Figs. 4 and 5.

end. Although (as has been known for some time [29]) there is also some probability of pinning in a Peierls-Nabarro well in bulk, the amount of emitted radiation is much larger during reflection, and most kinks may be expected to be trapped at the system boundary and converted into surface modes after having traveled along the chain once or more times.

This effect prevents the permanent movement of the system as a whole, which may be important for the physics of dislocations in solids. Kukushkin and Osipov [14] studied the continuous SG equation as a model for dislocation kink dynamics in thin films. They pointed out that such a kink dynamics explains qualitatively the experimentally observed effect of cluster migration [34,35], but results in an infinite diffusion coefficient. As we have shown, nonintegrability provides the neccessary dissipation mechanism. Note that this mechanism is inherent to the system and not related to external forces, impurities, etc.

On the other hand, in biological systems the idea of system movement as a whole has no sense. Instead, transport of energy and charge (protons in hydrogen bonds) within the chain is of interest. The kink trapping effect provides the possibility of locking the proton sublattice of the hydrogen bonded chain in a specific configuration after one kink passage, thus enabling effective proton transport. In addition, energy becomes localized at the system end for a relatively long time before it is radiated out.

It is important to note that the FK system is very special in at least two respects: it is exactly integrable in the continuum limit, and it does not support kink internal modes, except in a narrow range of parameters [31].

Exact integrability is a special property of a narrow class of models that cannot be expected in real systems. On the other hand, it should be stressed that actually it is *nonintegrability* and not discreteness that underlies the inelasticity of kink reflection (cf. the comparison of two discrete models in Ref. [25]), although growing discreteness enhances the effects of nonintegrability. Thus kink trapping at the system surface may be typical of a general class of systems, including continuous ones.

Another aspect of exact integrability of the SG model is the existence of breathers in continuous systems. In general, nonintegrable systems, breathers may exist only if the degree of discreteness is high enough [36]. Therefore, no stable surface modes may exist in such systems close to the continuum limit, unless the system properties are modified at its end [37]. Thus the free kink–surface state transition may have different properties in other models, where the final surface state is instable.

Recently it was shown [38] that even a small perturbation to an integrable equation results in the appearance of internal modes. The existence of such modes leads to many intriguing phenomena when kink-antikink collisions are considered, even in continuous models [39–41]. The dynamics of a finite system will therefore also be complex. All these phenomena are missed when the FK model is considered.

In spite of these special features of the FK (SG) model, the phenomenon of kink trapping may be expected to appear in any nonlinear Klein-Gordon system (ϕ^4, double-Morse [42]). Most such systems are nonintegrable even in the continuum limit, and support shape modes which will increase the number of possible dynamical scenarios. Nonetheless, in any of such models discreteness increases radiation both during normal kink motion and at reflection, leading to increasing trapping effects for larger amplitudes of the on-site potential.

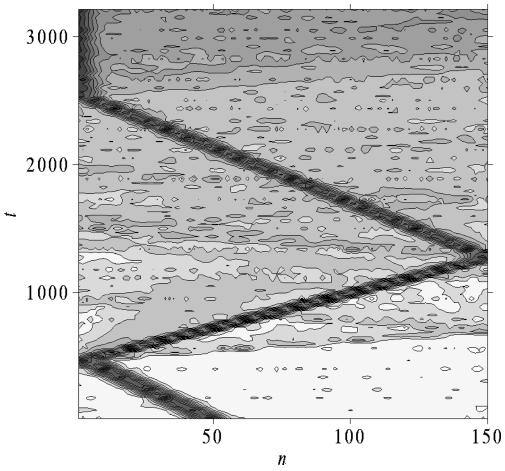

FIG. 7. Energy density diagram of the system dynamics for $a=0.01, V_0=0.6$, and initial kink velocity $v=-0.1$. The gray scale corresponds to the logarithm of the energy density, and is the same as in previous figures. Note that the kink accelerates at the first collision, but does not slow down at the second one: there is no transition into an antikink.

In our discussion we neglected the misfit between the nearest neighbor interaction and the period of the substrate potential. The results may easily be generalized for nonzero misfit, values lower than the critical misfit, above which the ground state of the system contains kinks. For $a>0$, kinks $[u'(x)>0]$ have lower energy than antikinks (the opposite is true for $a<0$). Therefore, reflections with kink $\rightarrow$ antikink transition lead to energy gain and kink acceleration (see Fig. 7). Due to radiative loss the kink usually has too little energy to transform back into an antikink when it arrives at the opposite end. Therefore, it reflects without transition or is trapped. Thus nonzero misfit introduces the additional effect of asymmetry between a kink and antikink and between the two kinds of reflections, but it does not otherwise influence the effects described above.

It may be noted that in the general case of $a\neq 0$ there is no mirror symmetry, and the equivalence between finite and infinite systems no longer holds. Thus the continuum results of Refs. [11] and [14] actually correspond to the zero-misfit case. The zero-tension condition of Frank and van der Merwe [2] would not be satisfied in the center of a symmetric solution (breather or kink-antikink) for $a\neq 0$.

Finally, let us note that the dynamics of finite FK-type systems in higher dimensions may be reduced to the dynamics of infinite systems with appropriate symmetry. Hence, the existence of nonlinear surface modes is guaranteed by theorems on the existence of breathers, provided that the discreteness is high enough [43,44].

V. CONCLUSION AND OUTLOOK

We have shown that unlike in the continuous model, in the discrete case a free kink may become trapped at the end of a chain due to inealistic scattering from the chain end. The

probability of such an effect is considerably higher than that of pinning in a PN potential well. In particular, we have shown that slow kinks always get stuck at the system end, whereas faster ones may be reflected with some loss of energy depending on the system discreteness (the potential amplitude V_0 in our system). Since fast kinks radiate energy and their speed drops very quickly below the (discreteness-dependent) critical velocity, the kink energy is also limited. We have found out that, for $V_0 \approx 0.8$, even kinks moving with this maximal velocity cannot be reflected; hence all kinks are transformed in bound surface states. This behavior may be interpreted in terms of both dislocation dynamics its described by the FK model and nonlinear transport phenomena, including those in biological systems.

It seems reasonable to continue the study in two directions: (1) Higher values of misfit might be included to make the model more realistic in its description of dislocation dynamics. (2) Other models (φ^4, double-Morse) might be analyzed to study the effect of nonintegrability in the continuum limit and of the existence of shape modes. Numerical verification of existence of higher-dimensional surface modes would also be very interesting.

ACKNOWLEDGMENTS

The authors are very grateful to Andrzej Radosz for a critical reading of the manuscript, and for many helpful comments. P. Machnikowski was supported by the Polish State Committee for Scientific Research under Grant No. 2 P03B 089 14.

APPENDIX

We will show here that if the initial condition has the symmetry (3), then this symmetry is conserved during the time evolution. Indeed, in new coordinates $\zeta_n = (u_n - u_{-n+1})/2, \eta_n = (u_n + u_{-n+1})/2$, the equations of motion have the forms

$$\ddot{\zeta}_n = \Delta_2 \zeta_n - \tfrac{1}{2} V'(\eta_n + \zeta_n) + \tfrac{1}{2} V'(\eta_n - \zeta_n),$$

$$\zeta_n(0) = 0, \quad \dot{\zeta}_n(0) = 0,$$

$$\ddot{\eta}_n = \Delta_2 \eta_n - \tfrac{1}{2} V'(\eta_n + \zeta_n) - \tfrac{1}{2} V'(\eta_n - \zeta_n),$$

$$\eta_n(0) = \eta_n^{(0)}, \quad \dot{\eta}_n(0) = \eta_n^{(1)}.$$

These equations obviously have a solution with $\zeta_n(t) \equiv 0$ and $\eta_n(t)$, satisfying

$$\ddot{\eta}_n = \Delta_2 \eta_n - V'(\eta_n), \quad \eta_n(0) = \eta_n^{(0)}, \quad \dot{\eta}_n(0) = \eta_n^{(1)}.$$

By its uniqueness, such a symmetric solution is the only possible one.

[1] Y. Frenkel and T. Kontorova, Zh. Eksp. Teor. Fiz. **8**, 1340 (1938) [Sov. Phys. JETP **13**, 1 (1938)].
[2] F. Frank and J. van der Merwe, Proc. R. Soc. London, Ser. A **198**, 205 (1949); **198**, 216 (1949); **200**, 125 (1949).
[3] A. Scott, in *Solitons and Condensed Matter Physics*, edited by A. Bishop and T. Schneider (Springer-Verlag, Berlin, 1978), p. 301.
[4] A. Davydov, *Solitony v Moliekuliarnykh Sistiemakh* (Naukova Dumka, Kiev, 1988) [*Solitons in Molecular Systems* (Reidel, Boston, 1985)].
[5] T. Dauxois, M. Peyrard, and A. R. Bishop, Phys. Rev. E **47**, 684 (1993).
[6] G. Gaeta, C. Reiss, M. Peyrard, and T. Dauxois, Riv. Nuovo Cimento **17**, 1 (1994).
[7] J. J. Ting and M. Peyrard, Phys. Rev. E **53**, 1011 (1996).
[8] G. Lamb, *Elements of Soliton Theory* (Wiley, New York, 1980).
[9] R. Hirota, J. Phys. Soc. Jpn. **33**, 1459 (1972).
[10] G. Bowtell and A. E. Stuart, Phys. Rev. B **15**, 3580 (1977).
[11] A. S. Kovalev, Fiz. Tverd. Tela (Leningrad) **21**, 1729 (1979) [Sov. Phys. Solid State **21**, 991 (1979)].
[12] G. Costabile *et al.*, Appl. Phys. Lett. **32**, 587 (1978).
[13] A. Pawełek, Acta Phys. Pol. A **68**, 815 (1985).
[14] S. Kukushkin and A. Osipov, Surf. Sci. **329**, 135 (1995).
[15] I. Markov and V. Karaivanov, Thin Solid Films **65**, 361 (1980).
[16] O. Braun, Surf. Sci. **230**, 262 (1990).
[17] S. Sharma, B. Bergersen, and B. Joos, Phys. Rev. B **29**, 6335 (1984).
[18] Y. Braiman, J. Baumgarten, J. Jortner, and J. Klafter, Phys. Rev. Lett. **65**, 2398 (1990).
[19] S. Stoyanov and H. Müller-Krumbhaar, Surf. Sci. **159**, 49 (1985).
[20] T. Watanabe and S. Takeno, J. Phys. Soc. Jpn. **63**, 2028 (1994).
[21] R. Wallis, A. Franchini, and V. Bortolani, Phys. Rev. B **50**, 9851 (1994).
[22] D. Bonart, A. Mayer, and U. Schröder, Phys. Rev. B **51**, 13 739 (1995).
[23] A. Franchini, V. Bortolani, and R. Wallis, Phys. Rev. B **53**, 5420 (1996).
[24] S. Dmitriev, L. Nauman, A. Wusatowska-Sarnek, and M. Starostenkov, Phys. Status Solidi B **201**, 89 (1997).
[25] K. Ø. Rasmussen, D. Cai, A. Bishop, and N. Grønbech-Jensen, Phys. Rev. E **55**, 6151 (1997).
[26] A. Pawełek, M. Jaworski, and J. Zagrodziński, J. Phys. A **21**, 2727 (1988).
[27] R. Boesch and M. Peyrard, Phys. Rev. B **43**, 8491 (1991).
[28] C. Willis, M. El-Batanouny, and P. Stancioff, Phys. Rev. B **33**, 1904 (1986).
[29] J. Currie, S. Trullinger, A. Bishop, and J. Krumhansl, Phys. Rev. B **15**, 5567 (1977).
[30] R. Boesch, C. Willis, and M. El-Batanouny, Phys. Rev. B **40**, 2284 (1989).
[31] O. M. Braun, Y. S. Kivshar, and M. Peyrard, Phys. Rev. E **56**, 6050 (1997).
[32] http://www.santafe.edu/projects/swarm
[33] D. Duncan, C. Walshaw, and J. Wattis, in *Nonlinear Coherent Structures in Physics and Biology*, edited by M. Remoissenet

and M. Peyrard (Springer-Verlag, Berlin, 1991), p. 151.
[34] J. Hamilton, M. Daw, and S. Foiles, Phys. Rev. Lett. **74**, 2760 (1995).
[35] S. Wang and G. Ehrlich, Phys. Rev. Lett. **79**, 4234 (1997).
[36] S. Flach and C. Willis, Phys. Rep. **295**, 181 (1998).
[37] Y. S. Kivshar, F. Zhang, and S. Takeno, Physica D **113**, 248 (1998).
[38] Y. S. Kivshar, D. E. Pelinovsky, T. Cretegny, and M. Peyrard, Phys. Rev. Lett. **80**, 5032 (1998).
[39] D. K. Campbell, J. F. Schonfeld, and C. A. Wingate, Physica D **9**, 1 (1983).
[40] M. Peyrard and D. K. Campbell, Physica D **9**, 33 (1983).
[41] D. K. Campbell, M. Peyrard, and P. Sodano, Physica D **19**, 165 (1986).
[42] H. Konwent, P. Machnikowski, and A. Radosz, J. Phys.: Condens. Matter **8**, 4325 (1996).
[43] S. Flach, Physica D **113**, 184 (1998).
[44] R. MacKay and S. Aubry, Nonlinearity **7**, 1623 (1994).